

Autonomous regeneration of concrete structures by incorporation of self-healing mechanisms

De Belie N.¹, Van Tittelboom K.¹, Tsangouri E.^{2,3}, Karaiskos G.², Snoeck D.¹, Wang J.^{1,3}, Araújo M.^{1,3} and Van Hemelrijck D.²

¹ Magnel Laboratory for Concrete Research, Ghent University, Technologiepark 904, 9052 Zwijnaarde, Belgium

² Department Mechanics of Materials and Constructions (MeMC), Vrije Universiteit Brussel (VUB), Pleinlaan 2, 1050 Brussel, Belgium

³ SIM vzw, Technologiepark 935, 9052 Zwijnaarde, Belgium

ABSTRACT

As an alternative to the usual strategy of manual repair of concrete cracks as they arise, concrete elements can be designed with an incorporated self-healing mechanism. Crack initiation will trigger the self-healing activity; the repair components are transported towards the location of damage and should heal the crack efficiently. Depending on the type of structure and the loading situation, the healing material should be able to heal a static or dynamic crack, and should provide mere crack filling, a regain in liquid-tightness or recovery of (some of the) mechanical properties.

Therefore different self-healing strategies were developed, including stimulated autogenous healing by introduction of superabsorbent polymers; autonomous healing by encapsulated calcium carbonate precipitating bacteria; and autonomous healing by an encapsulated polyurethane-based healing agent. These systems were first tested at laboratory scale for their effects on concrete properties and self-healing efficiency. Additionally, a large scale lab test was performed on self-healing concrete beams of 150 mm x 250 mm x 3000 mm, loaded in 4-point bending mode. Crack formation was monitored with a linear variable differential transformer, acoustic emission, digital image correlation and ultrasonic wave propagation technique based on embedded piezoelectric transducers. Crack healing was followed with crack microscopy and water ingress measurements.

INTRODUCTION

All strategies developed over the past 20 centuries to improve the strength and reliability of materials, are ultimately based on the paradigm of “damage prevention”, i.e. the materials are designed in such a way that the damage as a function of load and/or time is postponed as much as possible. The damage level here will never go down spontaneously. In recent years, however, it has been realized that an alternative strategy can be followed to make materials effectively stronger and more reliable, and that is by “damage management”, i.e. these materials have a built-in capacity to repair the damage incurred during use. When cracks form, the material itself is capable of “self-healing” the crack and restoring the functionality of the material (van der Zwaag, 2007).

Although there are very few applications on the market today, such as self-repairing clear coats for car surfaces and self-healing rubbers, it is expected that applications of the self-healing concept will show up in all industries. The program on Engineered Self-Healing Materials (SHE), and more specifically the project “Self-healing cementitious and mineral building materials” (SECEMIN), allowed Flanders to take a leading position in this fast developing area, in relation to the ambition to make Flanders a valuable player in the field, to develop new self-healing materials and to create new industrial activities. Three main self-healing methodologies were studied in SECEMIN: self-healing through superabsorbent polymers (SAPs) or hydrogels, through encapsulated prepolymers, and through calcium carbonate precipitating micro-organisms. The first two mechanisms will be discussed in this paper.

Superabsorbent polymers (SAPs) have the feature to absorb up to 500 times their own weight in aqueous solutions due to osmotic pressure, resulting in the formation of a hydrogel. The SAPs are long chains of linear polymers which are interconnected at several points. Nowadays, they are used in the hygiene and medical industry as care articles or smart pills, and they can also be used for firefighting or food

packaging. It was only a matter of time until this polymer also found its way as an additive in cementitious materials. SAPs can be used in cementitious materials for reducing the autogenous shrinkage, for changing the rheology of the fresh material, for increasing the freeze/thaw resistance, for self-sealing and even to promote autogenous healing. The latter can be explained as follows (Snoeck et al., 2012 & 2014). When cracking occurs, SAPs are exposed to the humid environment and swell. This swelling reaction seals the crack from intruding potentially harmful substances. Furthermore, especially mixtures where microfibers are introduced to restrict the crack width, show good healing efficiency. This means that the cracks will also be permanently healed, even if the humidity decreases again. These mixtures show multiple cracking and a high ductility. Many small cracks are formed (20-100 μm), which are possible to heal by autogenous healing which is stimulated by the presence of the SAP. Regain in mechanical properties upon crack healing was investigated by performance of four-point-bending tests on mortar beams and the sealing capacity of the SAP particles was measured through a decrease in water permeability. In an environment with a relative humidity of more than 60%, only samples with SAP showed healing. Introducing 1 m% of SAP gives the best results, considering no reduction of the mechanical properties in comparison to the reference, and the superior self-sealing capacity (Snoeck et al., 2012 & 2014).

Another crack repair approach makes use of embedded encapsulated polymer based healing agents. At the moment a crack appears, the capsules break and the healing agent is released. Upon contact with a second component which is provided by additional capsules, or with the air, the healing agent hardens and closes the crack against the ingress of water and other aggressive substances. As a proof of concept, in our previous research amongst others polyurethane prepolymers were inserted in concrete samples, protected by glass or ceramic tubes (Van Tittelboom et al., 2011 & 2013). It appeared possible to reduce the water permeability of cracked concrete by providing encapsulated healing agent but the healing efficiency greatly depended on the amount of cracks formed, on the developed crack width and especially on the amount of cracks crossing capsules and causing leaching of healing agent (Van Tittelboom et al., 2014).

In the current paper, the application of these two techniques to obtain self-healing was tested in a large scale test. Non-destructive techniques were applied to evaluate crack formation and healing.

MATERIALS AND METHODS

Concrete beams with(-out) self-healing properties. The self-healing techniques with SAP and PU respectively were implemented in a large-scale lab test to validate the small scale results and to further evaluate the best measuring and monitoring techniques. In order to prepare the element where self-healing was obtained by release of polyurethane from embedded capsules, about 350 glass capsules were filled with a polyurethane based healing agent. To position the tubes within the mould a network of plastic wires was attached through the walls of the mould (Figure 1.A). Glass tubes were glued onto this network of wires. Next to the capsules, this beam contained four reinforcement bars with a diameter of 10 mm. For the second self-healing approach under investigation, being the use of SAPs to cause crack sealing and promote autogenous crack healing, no additional preparation was needed. As SAPs are added at the moment of concrete mixing, for this beam, similar as for the reference beam (code: 'REF') only the four reinforcement bars were placed beforehand into the moulds (Figure 1.B).

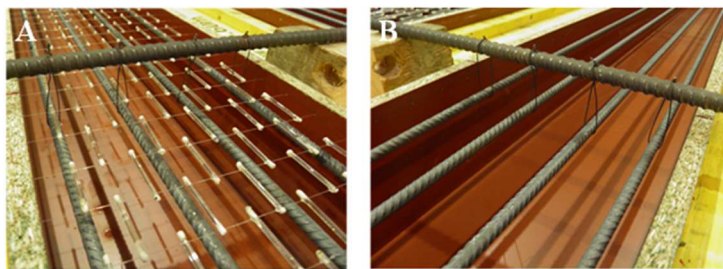


Figure 1. Preparation of beams with self-healing properties. (A) Placement of glass capsules with embedded healing agent onto a network of wires. (B) Position of the reinforcement bars within the mould.

Depending on the self-healing approach under investigation, concrete batches with slightly different properties were made to prepare the concrete beams. As vibration with a needle would not be possible for the beam containing encapsulated healing agent, it was chosen to use self-compacting concrete (SCC) for all beams. The composition of each of the mixes is shown in Table 1. After mixing of the ingredients, the moulds of the beams having dimensions of 150 mm x 250 mm x 3000 mm were filled.

Table 1. Composition of the concrete mixes under investigation (- = not applicable).

Components	REF		PU		SAP	
	[kg/m ³]	[l/m ³]	[kg/m ³]	[l/m ³]	[kg/m ³]	[l/m ³]
Sand 0/5	853	-	853	-	853	-
Gravel 2/8	370	-	370	-	370	-
Gravel 8/16	328	-	328	-	328	-
CEM I 52.5 N	300	-	300	-	300	-
Limestone filler	300	-	300	-	300	-
Water	-	165	-	165	-	207
PCE superplast	-	3.33	-	3.00	-	12
SAP	-	-	-	-	3	-

Four-point bending tests for crack creation. In order to create multiple cracks, the beams were loaded in four-point bending at the age of 28 days. To facilitate the later performance of water permeability tests, the beams were loaded in upward direction (Figure 2). Besides the exerted load, the deformation of the beam was recorded during four-point bending. The average crack width was used as reference value during performance of the four-point bending tests. Therefore, a measurement frame was positioned at the top of the beam (tensile zone), symmetrically with respect to the middle (Figure 2). The total displacement within the area covered by this measurement frame was measured by an LVDT in horizontal position, which was connected to the frame.

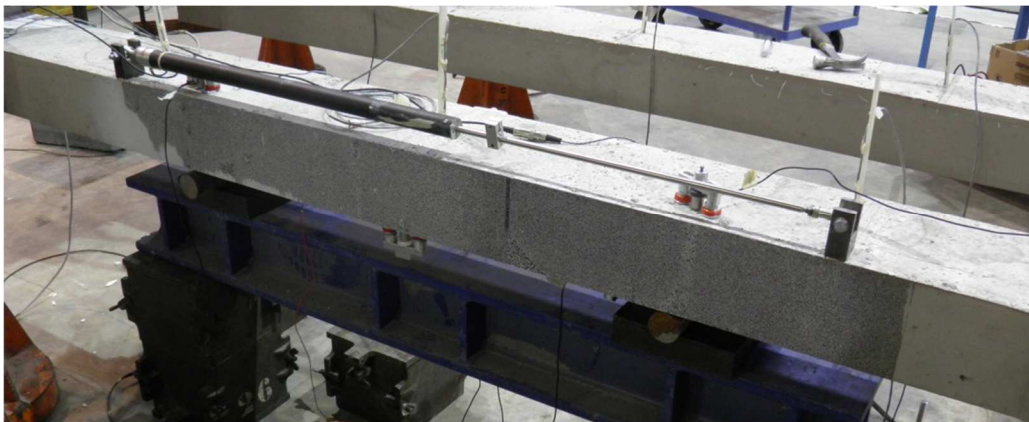


Figure 2. Test setup of the four-point bending test.

Beams were loaded in four-point bending until the average crack width as measured by the LVDT on the measurement frame amounted to 250 μm . Once this value was reached, the average crack width and the deformation of the beams were fixed. After a healing period of 7 weeks, the beams were unloaded.

Healing conditions. For the beam with encapsulated healing agent, crack formation triggered breakage of the capsules, release of the healing agent and subsequent crack repair when the healing agent came into contact with humidity in the concrete matrix. For the other approach under investigation contact with water is needed in order to activate the mechanism. As contact with water also promotes autogenous healing, it was decided to bring all beams (REF, PU, and SAP) in the same way in contact with water. Over a time span of 6 weeks, the beams were showered with water four times a day during one minute.

Evaluation of healing efficiency by microscopy. The crack width evolution over time was determined by means of microscopy. Therefore, crack widths were measured at fixed positions on the beams by means of an optical microscope. Measurements were repeated several times during the period of healing

in order to get an idea of the crack width evolution in time.

Evaluation of healing efficiency by water ingress tests. Evaluation of the crack healing efficiency was done by performing measurements of the water ingress into (healed) cracks. In order to measure the water ingress into the cracks before and after healing, water basins were attached on top of the beams (Figure 3). When the test setup was completely filled with water, the time needed for the water level to move from the one indicated mark to the other due to water ingress into the crack, was measured. Water ingress measurements were performed onto the unhealed cracks, immediately after crack formation and onto the healed cracks.

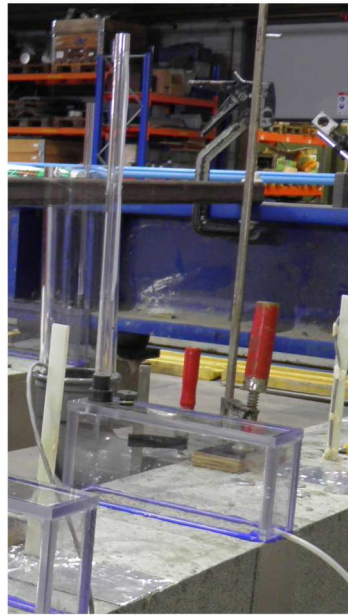


Figure 3. Setup of the water ingress test.

Non-destructive testing techniques to evaluate crack formation and crack healing. During performance of the four point bending tests Digital Image Correlation (DIC) was used to visualize the crack evolution. Two couples of high resolution CCD camera systems were placed facing the side of the beam. A speckle pattern was painted covering the middle bending zone of the samples (each of the DIC system monitored half of the area of analysis: $1200 \times 150 \text{ mm}^2$).

In addition, Acoustic Emission (AE) was applied to continuously monitor the bending fracture by means of registration of wave emissions. Eight resonant AE sensors were attached on the concrete surface by means of magnetic clamping systems. The AE sensors were placed at the middle zone of the sample where cracking was expected and formed a network that accurately located the sources of acoustic emission.

Both the DIC speckle patterns and the AE sensors location are schematically shown in Figure 4.

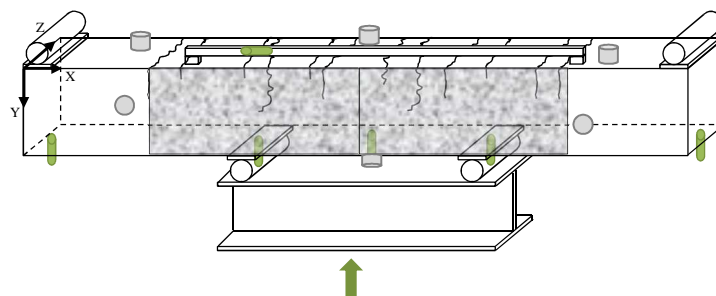


Figure 4. DIC and AE experimental setup of the four-point bending test; the black-white texture presents the DIC area of analysis, grey cylinders indicate the position of the AE sensors on the concrete sample surface and green cylinders are used to indicate the points where the deformation was measured with an LVDT.

Furthermore, an Ultrasonic Pulse Velocity (UPV) system was used, based on the FreshCon system which was initially designed for monitoring fresh concrete (Reinhart and Grosse, 2004). Based on the concept of 'smart aggregates' (Gu et al., 2006), a few PZT (lead-zirconate-titanate) piezoceramic transducers were designed and manufactured. A couple of these transducers were placed in each mould of the concrete beams in order to evaluate not only the gradual crack formation due to loading but also the possible partial healing and fracture recovery. The transducers were symmetrically to the centre of the beam fixed at a distance of 1400 mm in order to monitor the widest possible area of the cracked beams. In the present study, only compressional ultrasonic waves are used which are subject to a high level of complex reflections and scattering due to the constituent elements of concrete in the wave path. By the time the mechanical wave reaches the receiver, it is transformed into a complex waveform of which the early part mainly contains the contribution of a direct wave between the transducers and therefore carries information about the state of the microstructure in the direct path between the transducers. The damage index (d.i.) used in the study is therefore based on the early part of the received waves (Karaiskos et al., 2013): it is the root mean square deviation between the amplitude of the signal from the undamaged structure (before loading) and the signal from the damaged structure (during reloading), computed in the time window corresponding to the first half-period for the undamaged structure. This indicator is impacted both by the increase of the time of propagation and the decrease of amplitude of the received signal. When the amplitude of the received signal is too low or the wave arrives later than the tested period, then the damage index value is close to one.

RESULTS

Evaluation of healing efficiency by microscopy. Microscopic analysis of the beams (Figure 5) shows the different healing mechanisms. In the REF beam, autogenous healing occurred by the further hydration of cement particles and the precipitation of calcium carbonate after wet/dry cycles. In the PU beam, there was also some autogenous healing, but the main healing mechanism was autonomous healing due to the foaming action of the polyurethane in the crack, sealing it from intruding water. In the SAP beam, cracks are also closed due to autogenous healing, but superabsorbent polymers are able to stimulate it to a larger extent compared to the REF beam. Here, the polymers swell, take up the water during a wet period and gradually release it towards the matrix for a controlled formation of healing products.

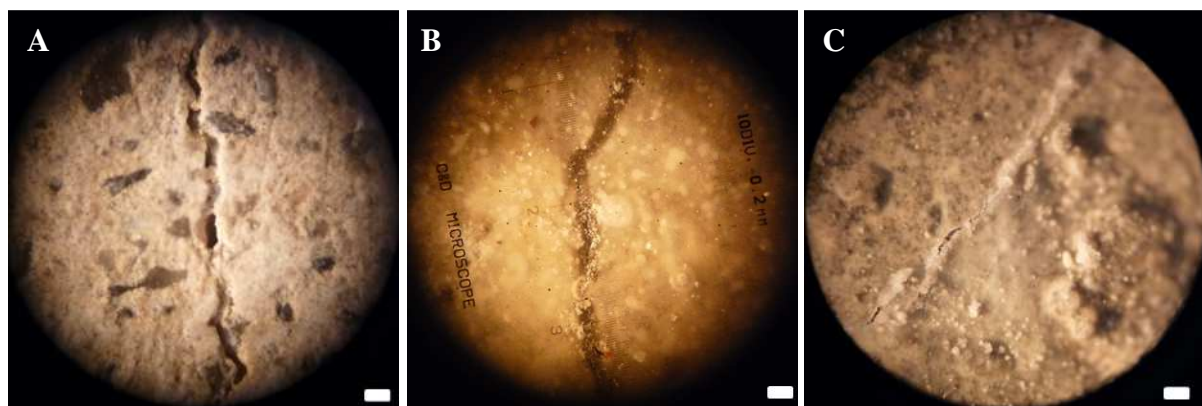


Figure 5. Micrographs of a crack in the REF beam (A), PU beam (B) and SAP beam (C) showing partial precipitation due to autogenous healing, autonomous healing by polyurethane and complete crack closure due to stimulated autogenous healing by means of superabsorbent polymers, respectively. The scale bar shows a distance of 200 μm .

The REF specimens, in which only autogenous healing takes place, show clear white crystals forming from the crack faces towards the centre of the crack as teeth-like structures. The whitish product is believed to be mainly composed of calcium carbonate.

Microscopic analysis of the cracks at the start and the end of the 7 weeks healing period allowed to calculate the crack closing ratio. This ratio was calculated by dividing the difference between the initial

and final crack width by the initial one. Analysis of the cracks at the top side of the REF beam resulted in a crack closing ratio of 26% which was similar as the ratio obtained for the beam with encapsulated polyurethane (23%). However, due to the fact that the presence of SAPs stimulates the autogenous healing capacity, the beam with embedded SAPs showed a significantly higher crack closing ratio of 60%.

As the obtained crack widths were relatively large, the cracks were not able to close completely in the REF beam, but the SAP beam showed better healing performance. This is mainly due to the controlled stimulation and precipitation of healing products in the crack. The PU healing mechanism is independent of the wet/dry cycles as most of the healing occurs within the first minutes after crack formation due to release of the embedded polyurethane. Additional autogenous crack healing only contributes to a limited extent to the healing efficiency of this series.

Evaluation of healing efficiency by water ingress tests. Before crack healing, the water ingress into the cracks of the beam with embedded SAPs was clearly higher compared to the ingress into the other series (Figure 6). This is due to the fact that the SAP particles within the matrix of this beam attract an additional amount of water. However, this will result in a beneficial effect later on, as the water, absorbed by the SAPs, will be released to the surrounding cementitious matrix and result in further hydration and calcium carbonate precipitation. When these newly formed crystals are precipitated inside the cracks this results in an increased autogenous crack healing efficiency.

This improved healing efficiency is partly represented by the results shown in Figure 5. While for the REF beam and the beam with encapsulated polyurethane (PU) higher water ingress values were obtained after healing, the SAP beam showed lower water ingress. We believe this should be attributed to healing of the cracks as for the SAP series crack closure was also shown from the microscopic analysis.

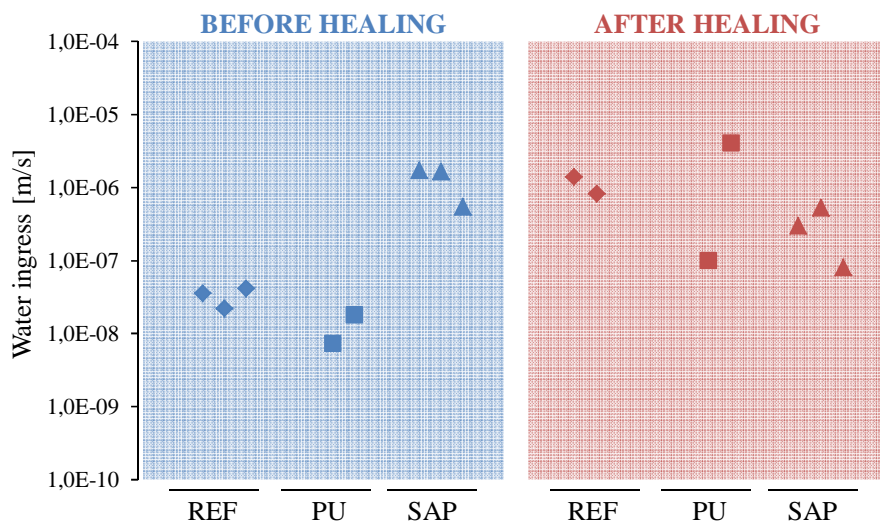


Figure 6. Water ingress [m/s] obtained for the cracks of the REF, PU and SAP beam before and after healing of the cracks.

The fact that higher water ingress was measured for the two other test series (REF and PU) is in contradiction with our expectations. However, we believe that this finding is due to the fact that the saturation state of the beams was different before and after healing. Moreover, these water ingress measurements were very difficult to perform as for some of the selected cracks water was not only intruding in the concrete matrix via the crack but also leaked out of neighbouring cracks. This makes it very difficult to draw sound conclusions from this test.

Detection of healing activation by Acoustic Emission when healing carriers rupture. The healing activation of the PU series can be detected by Acoustic Emission (Van Tittelboom et al., 2012, Tsangouri et al., 2013). In Figure 7, the acoustic emissions captured during testing of the PU beam are presented. The AE hits were classified based on the energy values. Every time that a brittle capsule ruptured, the eight AE sensors captured the emitted waves carrying high energy. At least 30 capsule breakage events

were detected confirming that healing agent was released into the crack. It was concluded that AE could accurately monitor the healing activation in the case a brittle encapsulation system was implemented.

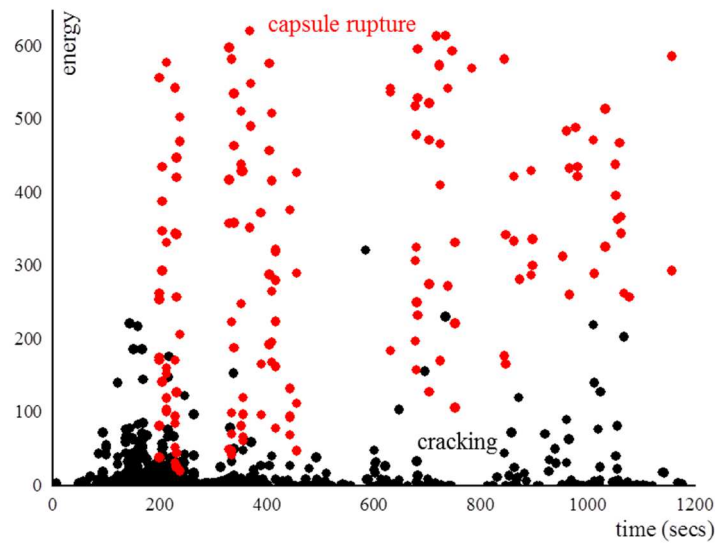


Figure 7. AE energy-based analysis detecting the capsule rupture (red dots) and cracking (black dots) events during loading.

Evaluation of crack formation and crack healing by Digital Image Correlation. The crack opening and propagation can be visualized by DIC during both loading and reloading test cycles. In Figure 8 the strain concentrations (strain ϵ_{xx} perpendicular to the loading direction) at the location of the cracks are presented. The DIC strain profiles allowed to locate several cracks along the beam length. The presence of PU and SAP material might change the crack distribution. To investigate that, the crack density was measured by means of DIC strain profiles showing that the reference beam carries 3.33 cracks/100mm along the side of the concrete beam, the PU healing beam carries 2.5 cracks/100 mm and finally the SAP healing beam carries 3 cracks/100 mm. It was observed that the presence of tubular capsules affected the crack evolution. The layer of tubes appeared to contribute as local reinforcing system that redistributed the microcracks leading to a slight decrease in crack numbers. The steel bars' movement masked the healing contribution as cracks re-open at reloading stage, since it was the source of great strain concentration (as shown in Figure 8 for the ϵ_{yy} strain profiles). Finally, the crack opening at the bottom of the tensile zone (where the cracks reach the greatest opening values) was measured during loading, unloading, reloading and at the end of testing. The mean values of crack opening (w in μm) are presented in Figure 9 for the three studied cases (REF, PU, SAP). Note that the average crack width, as measured by the LVDT on the measurement frame, covers both the sum of all crack widths and the elongation of the concrete. This is the reason why the estimated average crack width during loading (250 μm) is larger than what is actually determined with DIC. Comparing the REF series to both PU and SAP healing beam, it seems that the average crack widths were a bit larger for the REF than for the PU and SAP beams.

The graphs shown in Figure 10 demonstrate the excellent performance of the UPV technique based on embedded piezoceramic transducers for detecting the initiation and following the evolution of the cracking during the loading tests. There is a great repeatability of the graph patterns among the loading tests of the three concrete beams, which is well captured by the monitoring system. In all the three loading tests, the system is able to catch the initiation of damage as well as progressive and sudden damage events until complete failure.

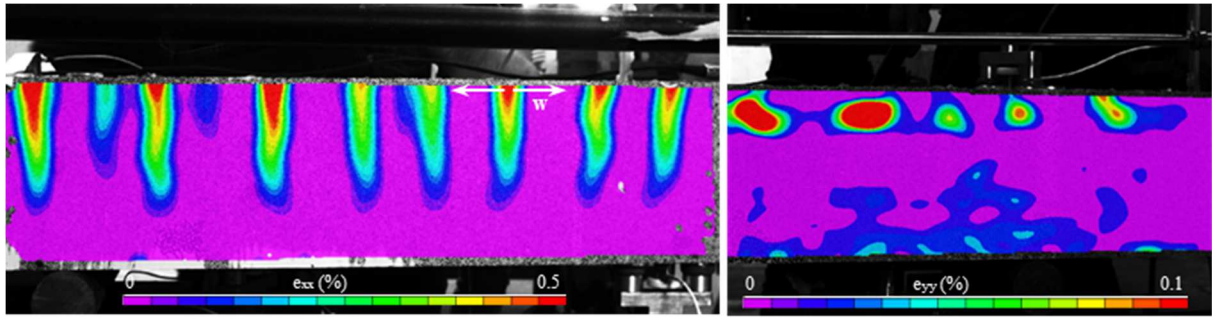


Figure 8. DIC strain profiles as captured at the end of testing visualising the crack evolution and the steel bars reinforcement movement due to yielding.

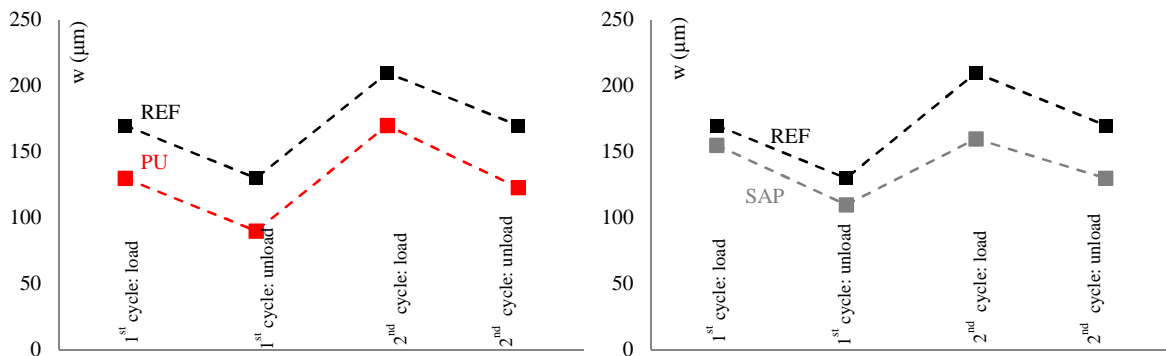


Figure 9. Mean values of DIC crack opening at the end of first and second loading cycles.

According to the received time signals during the loading tests of the beams, the damage index (d.i.) calculation could not be based anymore on the very early part of the measured waves (i.e. first half-period of the signal from the undamaged beam). The wave arrival time moved drastically to higher values, even at low loads. In all the previous applications of the present technique, the distance between the actuator and receiver(s) was up to 100 mm and a couple of cracks were created in that small area. In the present application, the great shift of the wave arrival time could be attributed to the great distance between the actuator and the receiver (i.e. 1400 mm), as well as to the creation of multiple cracks. As a consequence, the damage index calculation was now based on difference between the arrival times of the wave through the undamaged beam and the beam at maximum loading. This d.i. is very simple which makes it suitable for on-line monitoring applications. It is efficient to detect the appearance of damage and follow its evolution, but does not give a quantitative evaluation of that damage. It can therefore be used as an efficient tool to trigger alarms, after which other methods can be used to assess the severity of damage.

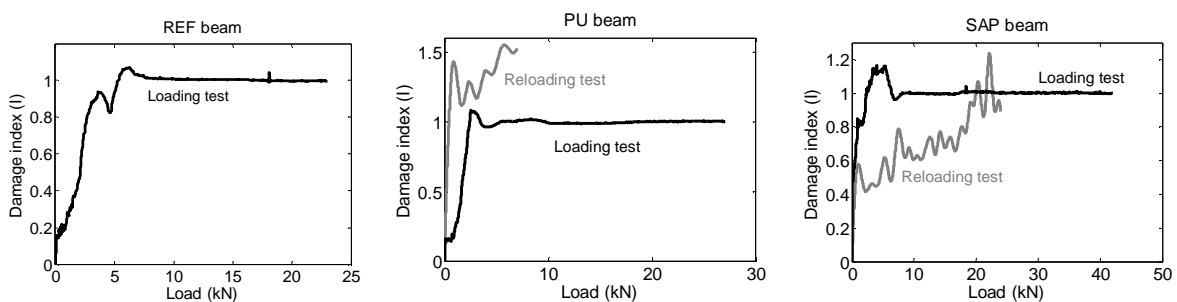


Figure 10. Evolution of the damage index as a function of the applied load for REF, PU and SAP beams during the loading and the reloading tests.

CONCLUSIONS

In our earlier research, three self-healing methodologies for concrete have been studied in detail at the laboratory scale: self-healing through superabsorbent polymers (SAPs) or hydrogels, through encapsulated prepolymers such as PU or PMMA, and through calcium carbonate precipitating micro-organisms. Currently efforts are made to scale up these mechanisms for use in concrete beams and plates. Not only the self-healing additives themselves, but also the monitoring methods have to be scaled up in order to evaluate the self-healing efficiency.

Two types of self-healing concrete beams of size 150 mm x 250 mm x 3000 mm were cast. One type contained brittle tubular capsules filled with a polyurethane based healing agent, glued onto a network of wires that was attached to the walls of the mould. The aim is that the tubes break when a crack appears, allowing the precursor to react and fill the crack with PU. A second type of self-healing beam contained 3 kg superabsorbent polymers (SAP) per m³ of concrete (equivalent to 1% of the cement weight). In this case when cracking occurs, SAP are exposed to the humid environment and swell. This swelling reaction seals the crack from intruding potentially harmful substances. Later on, the SAP will release its water to allow further hydration of unhydrated binder particles and precipitation of calcium carbonate in the crack.

These two beams, as well as a reference beam without self-healing additives, were loaded at the age of 28 days in four-point bending until the average crack width amounted to 250 µm. After a healing period of 7 weeks with regular water sprinkling, the beams were unloaded.

Microscopic monitoring allowed to visualise crack healing at the surface. Here, the beam with embedded SAPs showed a significantly higher crack closing ratio (60%) than the reference beam (crack closing ratio of 26% by autogenous healing).

Water ingress measurements to monitor the regain in water-tightness due to self-healing provided quite dubious results. It was very difficult to attach the water containers to the beam surface without leaks. Some water intruding in the concrete matrix via one crack also leaked out of neighbouring cracks. Furthermore, a varying level of water saturation of the beams affects the water ingress into the concrete matrix and therefore also the measurement results.

Acoustic emission measurements could accurately monitor the healing activation in the case a brittle encapsulation system was implemented. Digital image correlation allows to nicely visualise crack opening and propagation. The presence of tubular capsules affected the crack evolution, leading to a slight decrease in crack numbers. An UPV technique based on embedded piezoceramic transducers was useful for detecting the initiation and following the evolution of the cracking. For future tests, the distance between the actuator and the receiver(s) should be decreased, and it should be checked that no presence of water in the cracks would distort the results.

ACKNOWLEDGEMENTS

This research under the program SHE (Engineered Self-Healing materials) (project SECEMIN: Self-healing cementitious and mineral building materials) was funded by SIM (Strategic Initiative Materials in Flanders). The authors would like to thank the foundations for their financial support.

REFERENCES

- Reinhart, H. W., Grosse, C. U. (2004). Continuous monitoring of setting and hardening of mortar and concrete. *Construction Building Materials*, 18, 145-154.
- Gu, H., Song, G., Dhonde, H., Mo, Y.L., Yan, S. (2006). Concrete early-age strength monitoring using embedded piezoelectric transducers. *Smart Materials and Structures*, 15(6), 1837-1845.
- Karaiskos, G., Flawinne, S., Sener, J.-Y., Deraemaeker, A. (2013). Design and validation of embedded piezoelectric transducers for damage detection applications in concrete structures. 10th International Conference on Damage Assessment of Structures (DAMAS 2013), July 8th-10th, Trinity College Dublin, Ireland.
- Snoeck, D., Steuperaert, S., Van Tittelboom, K., Dubruel, P., De Belie, N. (2012). Visualization of water penetration in cementitious materials with superabsorbent polymers by means of neutron radiography. *Cement and concrete research*, 42,

1113-1121.

- Snoeck, D., Van Tittelboom, K., Steuperaert, S., Dubruel, P., De Belie, N. (2014, online 2012) Self-healing cementitious materials by the combination of microfibres and superabsorbent polymers. *Journal of Intelligent Material Systems and Structures*, 25(1), 13-24.
- Tsangouri, E., Aggelis, D., Van Tittelboom, K., De Belie, N., Van Hemelrijck, D. (2013). Detecting the Activation of a Self-Healing Mechanism in Concrete by Acoustic Emission and Digital Image Correlation. *The Scientific World Journal*, Article ID 424560, 10 pages, doi:10.1155/2013/424560.
- Tsangouri, E., Karaiskos, G., Aggelis, D., Deraemaeker, A., Van Hemelrijck, D. (2014). Crack sealing and damage recovery monitoring of a concrete healing system using embedded piezoelectric transducers. *Structural Health Monitoring journal*, accepted.
- Van der Zwaag, S. (2007) Self-Healing Materials: An Alternative Approach to 20 Centuries of Materials Science. Springer Series in Materials Science, ed. S. van der Zwaag. Vol. 100. 388p.
- Van Tittelboom, K., De Belie, N., Van Loo, D., Jacobs, P. (2011). self-healing efficiency of cementitious materials containing tubular capsules filled with healing agent. *Cement and concrete composites*, 33(4), 497-505.
- Van Tittelboom, K., De Belie, N., Lehmann, F., Grosse, C. (2012). Acoustic emission analysis for the quantification of autonomous crack healing in concrete. *Construction and building materials*, 28, 333-341.
- Van Tittelboom, K., Snoeck, D., Vontobel, P., Wittmann, F.H., De Belie, N. (2013). Use of neutron radiography and tomography to visualize the autonomous crack sealing efficiency in cementitious materials. *Materials and Structures*, 46(1), 105-121.
- Van Tittelboom, K., Tsangouri, E., Van Hemelrijck, D., De Belie, N. (2014). The efficiency of self-healing concrete using more realistic manufacturing procedures and crack patterns. *Cement and concrete composites*, in press.